Electronic supplementary information

for

Photocatalytic CO_2 reduction catalysed by 3d transition metal complexes bearing an S_2N_2 ancillary ligand equipped with pyridine pendants as a binding site for Lewis acids

Tomoya Ishizuka, Asuka Hamaguchi, Yuki Hayashi, Yuto Tsukakoshi, Hiroaki Kotani, Takuya Kawanishi and Takahiko Kojima*

Experimental section.

General.

Chemicals and solvents were purchased from commercial sources such as FUJIFILM Wako Chemicals, Tokyo Chemical Industry Co., and Sigma-Aldrich Co. and used as received unless otherwise mentioned. All synthetic reactions were performed under Ar atmosphere. ^{1}H NMR measurements were performed on a Bruker AVANCE 400 spectrometer. ESI-TOF-MS spectra were obtained on a JEOL JMS-T100CS mass spectrometer. Gas chromatography was performed using a Shimadzu GC-2014 gas chromatograph [Ar carrier, a packed column with molecular sieves 5A (3.0 m × 3.0 mm, 60 – 80 mesh) at 353 K] equipped with a thermal conductivity detector (TCD). UV-Vis spectroscopy was carried out on a Shimadzu UV-3600 spectrophotometer at room temperature using quartz cells. bpet (**1**)[1], bpet-py$_2$ (**2**)[2] and BIH (= 1,3-Dimethyl-2-phenyl-2,3-dihydro-1*H*-benzo[*d*]imidazole)[3] were synthesized according to the reported procedures.

Synthesis.

[Mn^{II}(bpet)(H$_2$O)$_2$](ClO$_4$)$_2$ ([1-Mn](ClO$_4$)$_2$). A solution of Mn(ClO$_4$)$_2$·6H$_2$O (0.87 g, 2.4 mmol) in methanol (20 mL) was added to a solution of **1** (0.67 g, 2.4 mmol) in methanol (20 mL) and the mixture was stirred for 1 d at room temperature under Ar. The mixture was evaporated and dried *in vacuo* and recrystallization of the solid obtained from acetonitrile/ethyl acetate gave colourless crystals of [**2**-Mn](ClO$_4$)$_2$ (1.09 g, 1.93 mmol, 80% yield). Anal. Calcd. for C$_{14}$H$_{16}$N$_2$S$_2$Mn·2ClO$_4$·1.5H$_2$O: C 30.17, H 3.44, N 5.03. Found: C 29.92, H 3.21, N 4.84. ESI-TOF-MS (CH$_3$CN): *m/z* = 429.92 (calcd. for [**1**-Mn – 2H$_2$O + ClO$_4$]$^+$: 429.96).

[Fe^{II}(bpet)(CH$_3$CN)$_2$](ClO$_4$)$_2$ ([1-Fe](ClO$_4$)$_2$). A solution of Fe(ClO$_4$)$_2$·6H$_2$O (0.54 g, 1.5 mmol) in methanol (10 mL) was added to a solution of **1** (0.41 g, 1.5 mmol) in methanol (20 mL) and the mixture was stirred for 1 d at room temperature under Ar. The mixture was evaporated and dried *in vacuo* and recrystallization of the solid obtained from acetonitrile/ethyl acetate gave purple crystals of [**1**-Fe](ClO$_4$)$_2$ (0.59 g, 0.96 mmol, 65% yield). Anal. Calcd. for C$_{14}$H$_{16}$N$_2$S$_2$Fe·2ClO$_4$·1.5CH$_3$CN: C 34.45, H 3.49, N 8.27. Found: C 34.35, H 3.46, N 8.38. ESI-TOF-MS (CH$_3$CN): *m/z* = 430.91 (calcd. for [**1**-Fe – 2CH$_3$CN + ClO$_4$]$^+$: 430.96).

[Co^{II}(bpet)(H$_2$O)$_2$](ClO$_4$)$_2$ ([1-Co](ClO$_4$)$_2$). A solution of Co(ClO$_4$)$_2$·6H$_2$O (0.36 g, 1.0

mmol) in methanol (10 mL) was added to a solution of **1** (0.27 g, 1.0 mmol) in methanol (20 mL) and the mixture was stirred for 15 h at room temperature under Ar. The resultant pale red precipitate was filtered and washed with MeOH. Recrystallization of the solid obtained from acetonitrile/ethyl acetate gave red crystals of [**1**-Co]$(ClO_4)_2$ (0.15 g, 0.24 mmol, 25% yield). Anal. Calcd. for $C_{14}H_{16}N_2S_2Co{\cdot}2ClO_4{\cdot}1.75H_2O$: C 29.72, H 3.47, N 4.95. Found: C 29.57, H 3.21, N 4.98. ESI-TOF-MS (CH_3CN): *m/z* = 433.89 (calcd. for [**1**-Co – $2H_2O$ + ClO_4]$^+$: 433.96).

[Mn(bpet-py$_2$)(H$_2$O)$_2$](ClO$_4$)$_2$ ([2-Mn](ClO$_4$)$_2$). **2** (10.4 mg, 0.023 mmol) and $Mn(ClO_4)_2{\cdot}6H_2O$ (8.20 mg, 0.023 mmol) were mixed in CH_3CN (2 mL) and the mixture was stirred at room temperature for 2 h. The solvent was evaporated and the resultant dull yellow solid was washed with ethyl acetate. Recrystallization of the solid obtained from acetonitrile/ethyl acetate gave dull yellow solid of [**2**-Mn]$(ClO_4)_2$ (8.86 mg, 14 μmol, 64%). Anal. Calcd. for $C_{26}H_{26}N_4S_2Mn{\cdot}2(ClO_4){\cdot}2(H_2O){\cdot}\ 0.5CH_3COOCH_2CH_3$: C 42.43, H 4.32, N 7.07. Found: C 42.60, H 4.15, N 7.22. ESI-TOF-MS (CH_3CN): *m/z* = 612.00 (sim for [**2**-Mn – $2H_2O$ + ClO_4]$^+$: 612.05).

[Fe(bpet-py$_2$)(H$_2$O)$_2$](ClO$_4$)$_2$ ([2-Fe](ClO$_4$)$_2$). Solutions of **2** (20.0 mg, 0.044 mmol) in absolute ethanol (4 mL) and $Fe(ClO_4)_2{\cdot}6H_2O$ (36.2 mg, 0.10 mmol) in absolute ethanol (8 mL) were mixed under Ar and the mixture was stirred at room temperature for 18 h. The resultant dull brown precipitate was filtered and washed with ethyl acetate. Recrystallization of the solid obtained from acetonitrile/ethyl acetate gave brown solid of [**2**-Fe]$(ClO_4)_2$ (6.00 mg, 9.8 μmol, 22%). Anal. Calcd. For [$C_{26}H_{26}N_4S_2Fe$-$2H^+$]$\cdot$ $4(ClO_4){\cdot}0.5CH_3COOCH_2CH_3$: C 35.09, H 3.37, N 5.85. Found: C 34.77, H 3.61, N 5.93. ESI-TOF-MS (CH_3CN): *m/z* = 612.93 (sim for [**2**-Fe – $2H_2O$ + ClO_4]$^+$: 613.04).

[Co(bpet-py$_2$)(H$_2$O)$_2$](ClO$_4$)$_2$ ([2-Co](ClO$_4$)$_2$). Solutions of **2** (10.5 mg, 0.023 mmol) in absolute methanol (2 mL) and $Co(ClO_4)_2{\cdot}6H_2O$ (8.54 mg, 0.023 mmol) in absolute methanol (2 mL) were mixed under Ar and the mixture was stirred at room temperature for 18 h. The resultant dull pink precipitate was filtered and washed with ethyl acetate. Recrystallization of the solid obtained from acetonitrile/ethyl acetate gave dull pink solid [**2**-Co]$(ClO_4)_2$ (12.8 mg, 21 μmol, 90%). Anal. Calcd. for [$C_{26}H_{26}N_4S_2Co$-H^+]$\cdot$ $3(ClO_4){\cdot}3(H_2O)$: C 36.19 H 3.78, N 6.28. Found: C 36.18, H 3.68, N 6.28. ESI-TOF-MS (CH_3CN): *m/z* = 616.11 (sim for [**2**-Co – $2H_2O$ + ClO_4]$^+$: 616.02).

X-ray Crystallography.

Single crystals of **1**-Fe·$(ClO_4)_2$ and **1**-Co·$(ClO_4)_2$, suitable for X-ray crystallography was obtained by recrystallization with vapour diffusion of AcOEt into their acetonitrile solutions. The axial ligands of **1**-Co were replaced with CH_3CN during recrustallization. A crystal of **1**-Mn·$(ClO_4)_2$ with low quality was also obtained by recrystallization with vapour diffusion of AcOEt into its acetonitrile solution. The crystals were mounted using a mounting loop. All diffraction data were collected on a Bruker APEXII diffractometer at 120 K with a graphite-monochromated Mo Kα radiation source (λ = 0.71073 Å) by the 2θ scan. The structure was solved by a direct method (SIR-97)[4] and expanded with a differential Fourier technique. All non-hydrogen atoms were refined anisotropically and the refinement was carried out with full-matrix least-squares on *F*. All calculations were performed using the Yadokari-XG crystallographic software package.[5] Crystallographic data for **1**-Fe·$(ClO_4)_2$, **1**-Co·$(ClO_4)_2$, and **1**-Mn·$(ClO_4)_2$ are summarized in Table S3. In the structure refinements, contribution of the solvent molecules of crystallization were subtracted from the diffraction pattern by the "Squeeze" program.[6]

References.

1. D. Hong, Y. Tsukakoshi, H. Kotani, T. Ishizuka and T. Kojima, *J. Am. Chem. Soc.,* 2017, **139**, 6538.
2. D. Hong, T. Kawanishi, Y. Tsukakoshi, H. Kotani, T. Ishizuka and T. Kojima, *J. Am. Chem. Soc.,* 2019, **141**, 20309.
3. X.-Q. Zhu, M.-T. Zhang, A. Yu, C.-H. Wang, J.-P. Cheng, *J. Am. Chem. Soc.,* 2008, **130**, 2501.
4. G. M. Sheldrick, SIR97 and SHELX97, University of Göttingen, Göttingen (Germany), 1997.
5. C. Kabuto, S. Akine, T. Nemoto, E. Kwon, *J. Cryst. Soc. Jpn.,* 2009, **51**, 218.
6. P. V. D. Sluis, A. L. Spek, *Acta Crystallogr.,* 1990, **A46**, 194.

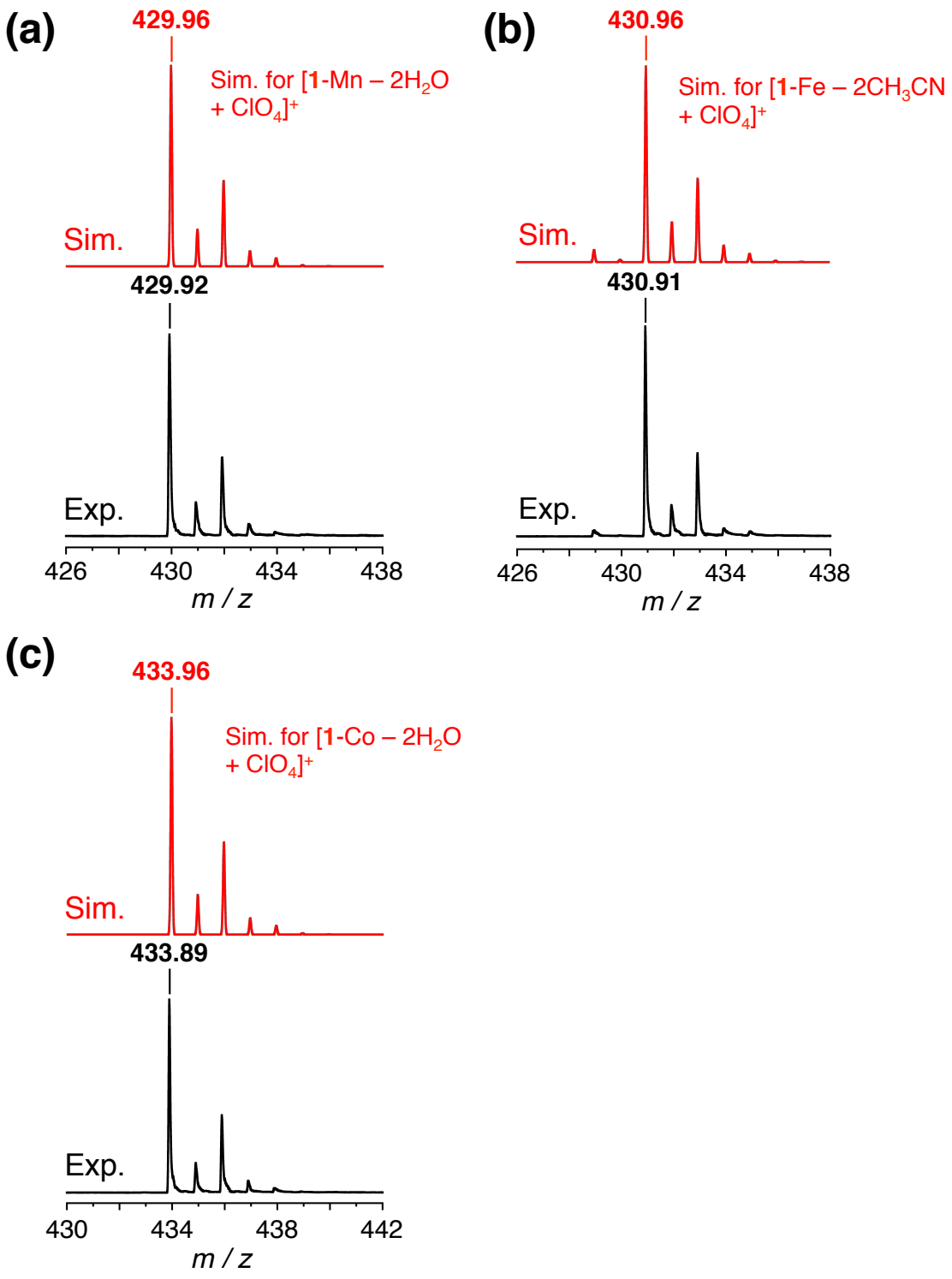

Fig. S1. ESI-TOF-MS spectrum of [**1**-Mn]$(ClO_4)_2$ (a), [**1**-Fe]$(ClO_4)_2$ (b), and [**1**-Co]$(ClO_4)_2$ (c) in CH_3CN.

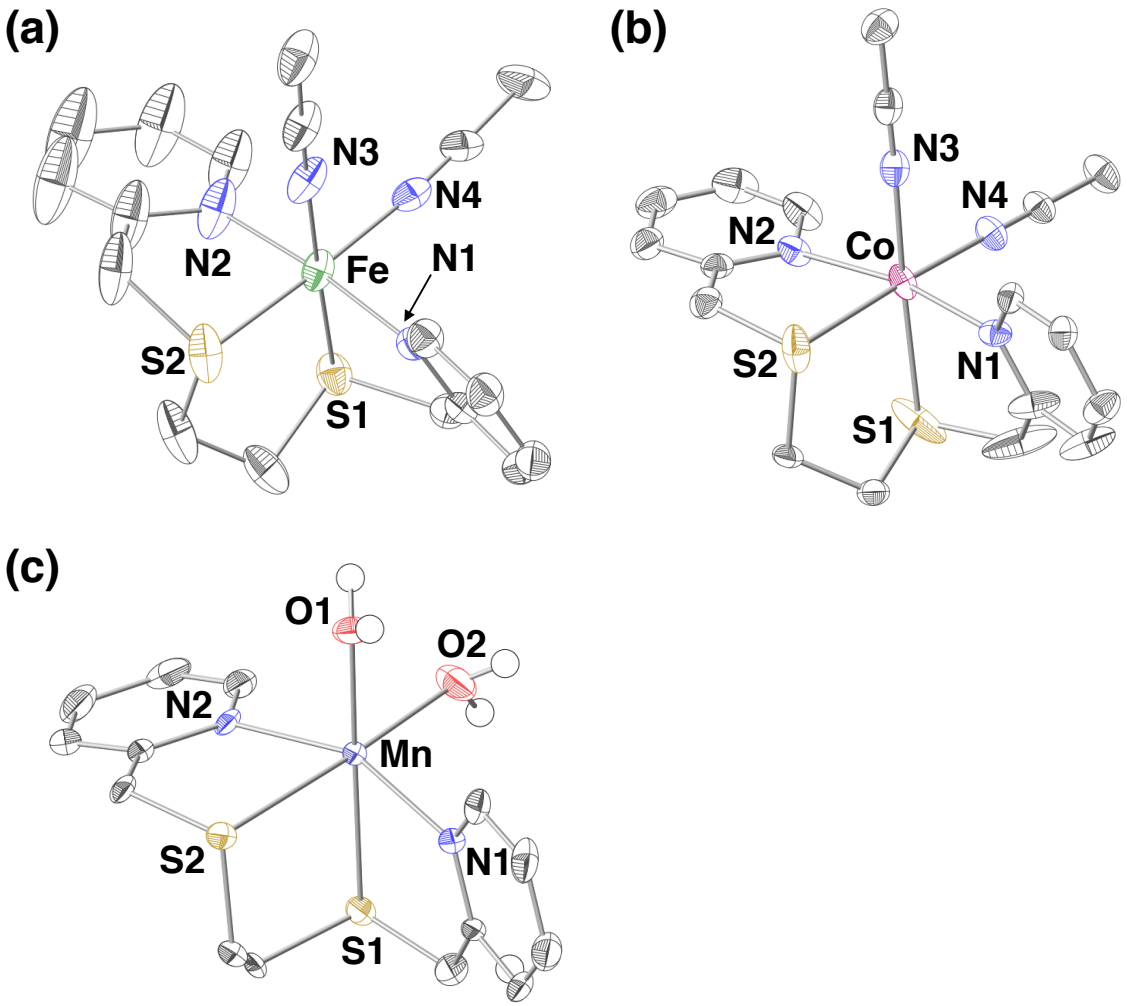

Fig. S2. Crystal structures of **1**-Fe (a), **1**-Co (Solv = CH_3CN) (b), and **1**-Mn (c). The thermal ellipsoids are drawn at the 50% probability level.

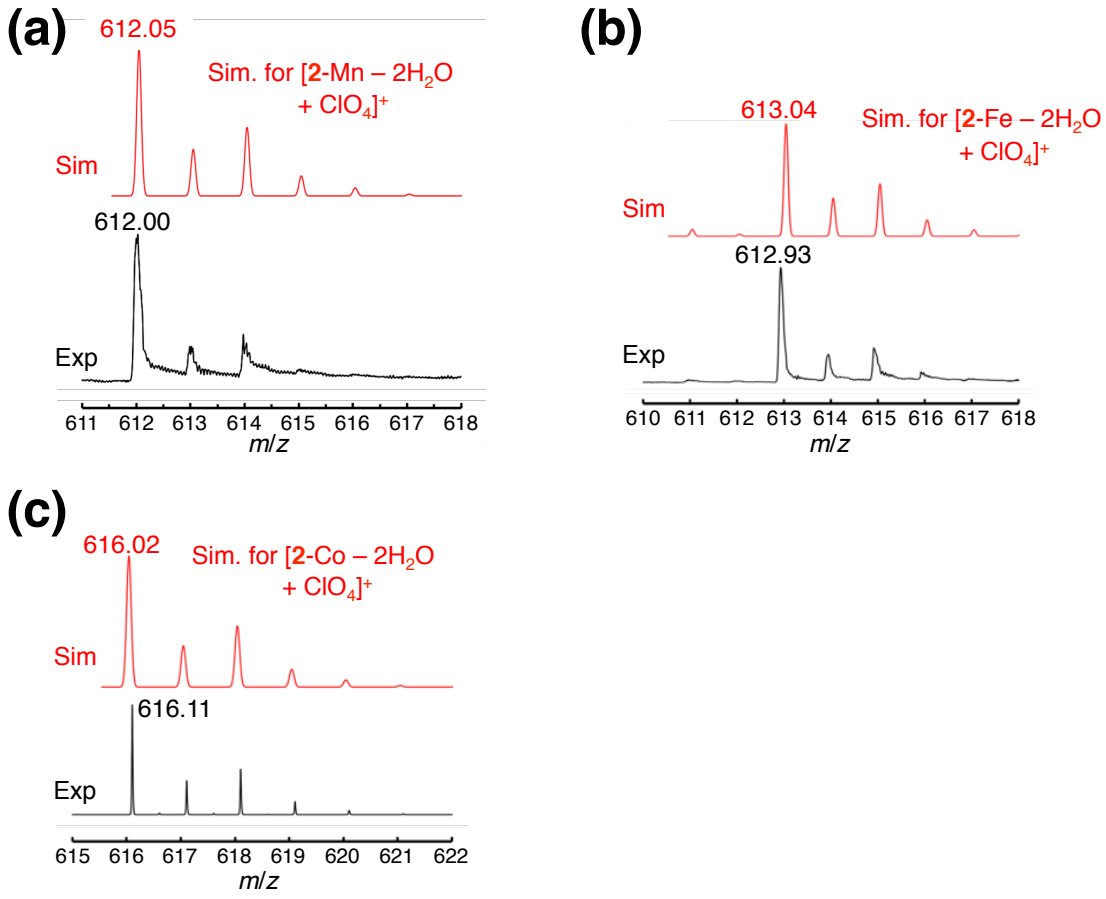

Fig. S3. ESI-TOF-MS spectrum of [**2**-Mn]$(ClO_4)_2$ (a), [**2**-Fe]$(ClO_4)_2$ (b), and [**2**-Co]$(ClO_4)_2$ (c) in CH_3CN.

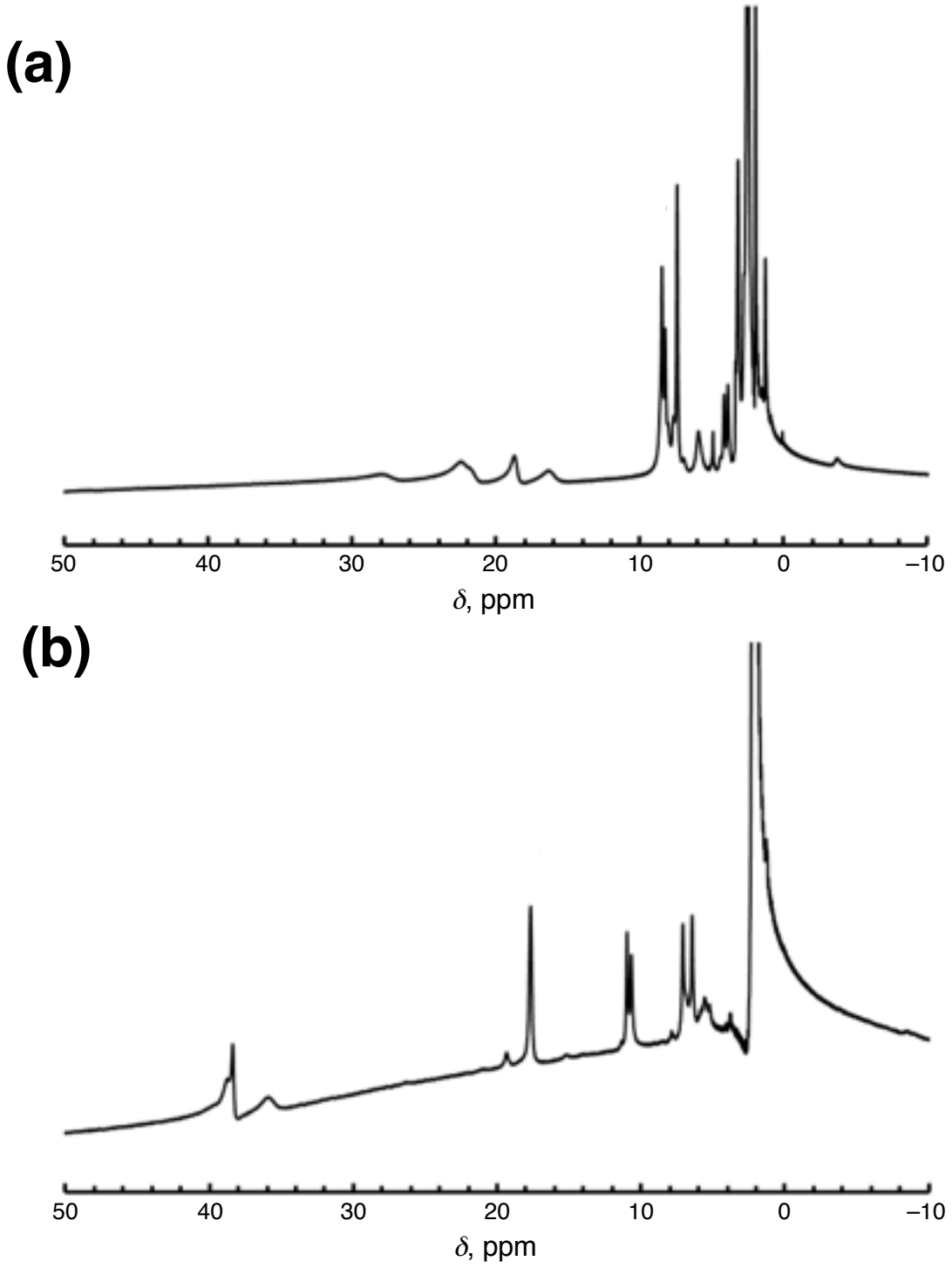

Fig. S4. ^{1}H NMR spectra of [**2**-Fe]$(ClO_4)_2$ (a), and [**2**-Co]$(ClO_4)_2$ (b) in CD_3CN.

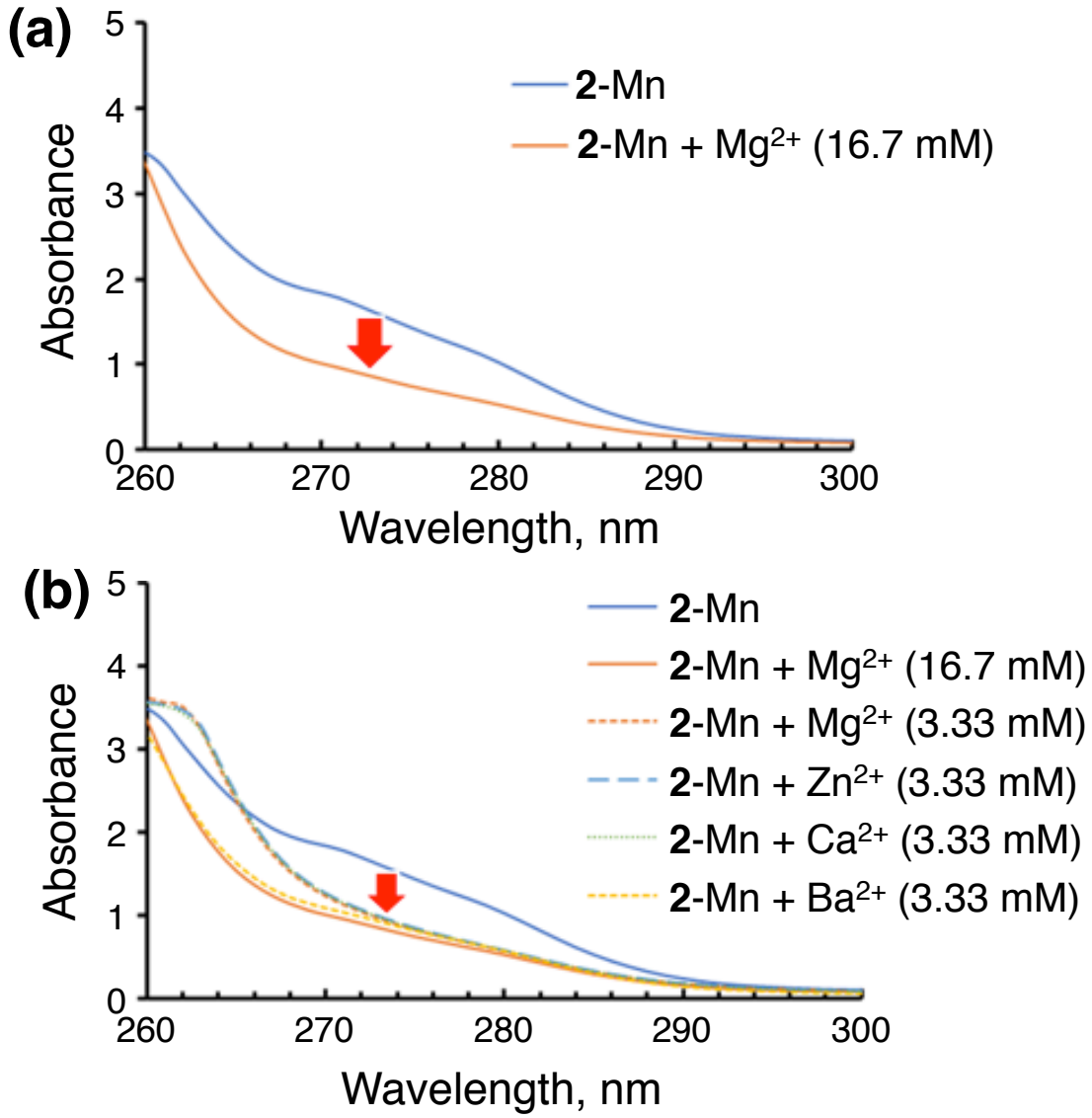

Fig. S5. UV-vis spectra of **2**-Mn (0.1 mM) in the absence and presence of $Mg(ClO_4)_2$ (a) and those of **2**-Mn (0.1 mM) in the absence or presence of perchlorate salts of Lewis-acidic metal ions (b) in a DMA/H_2O (9:1, v/v) mixed solvent at room temperature.

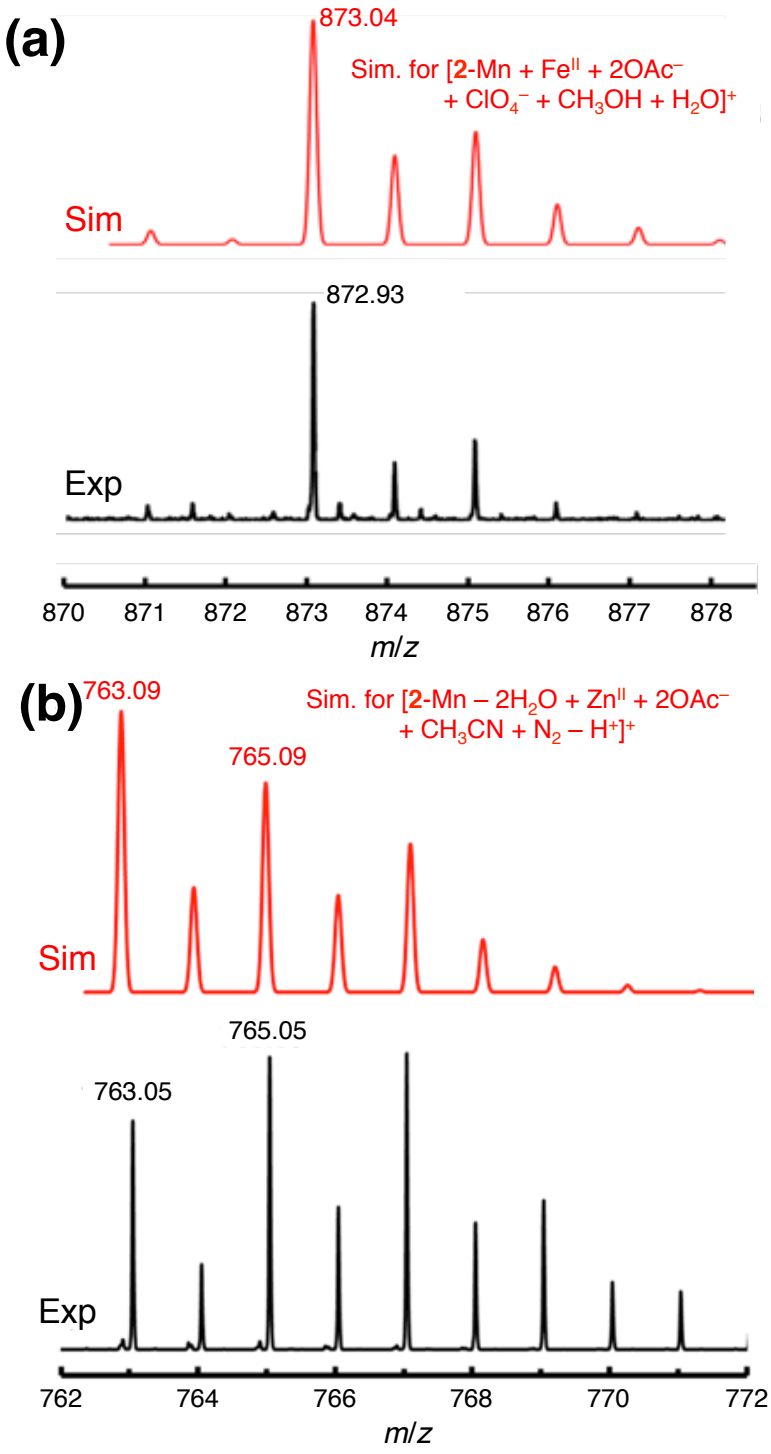

Fig. S6. (a) A peak cluster (black) assignable to Fe^{2+}-bound **2**-Mn, observed in the ESI-TO-MS spectrum of **2**-Mn in the presence of $Fe(OAc)_2$ (0.6 mM) in CH_3CN, and its simulation (red). (b) A peak cluster (black) assignable to Zn^{2+}-bound **2**-Mn (black), observed in the ESI-TO-MS spectrum of **2**-Mn in the presence of $Zn(OAc)_2$ (0.6 mM) in CH_3CN, and its simulation (red).

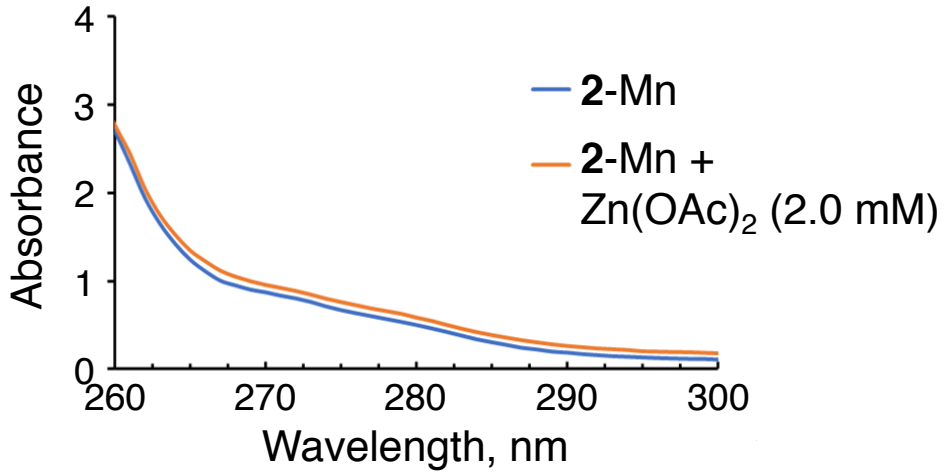

Fig. S7. UV-vis spectra of **2**-Mn (0.1 mM) in the absence (blue) and presence of $Zn(OAc)_2$ (2.0 mM; red) as a Lewis acid in DMA/H_2O (9:1, v/v) mixed solvent at room temperature.

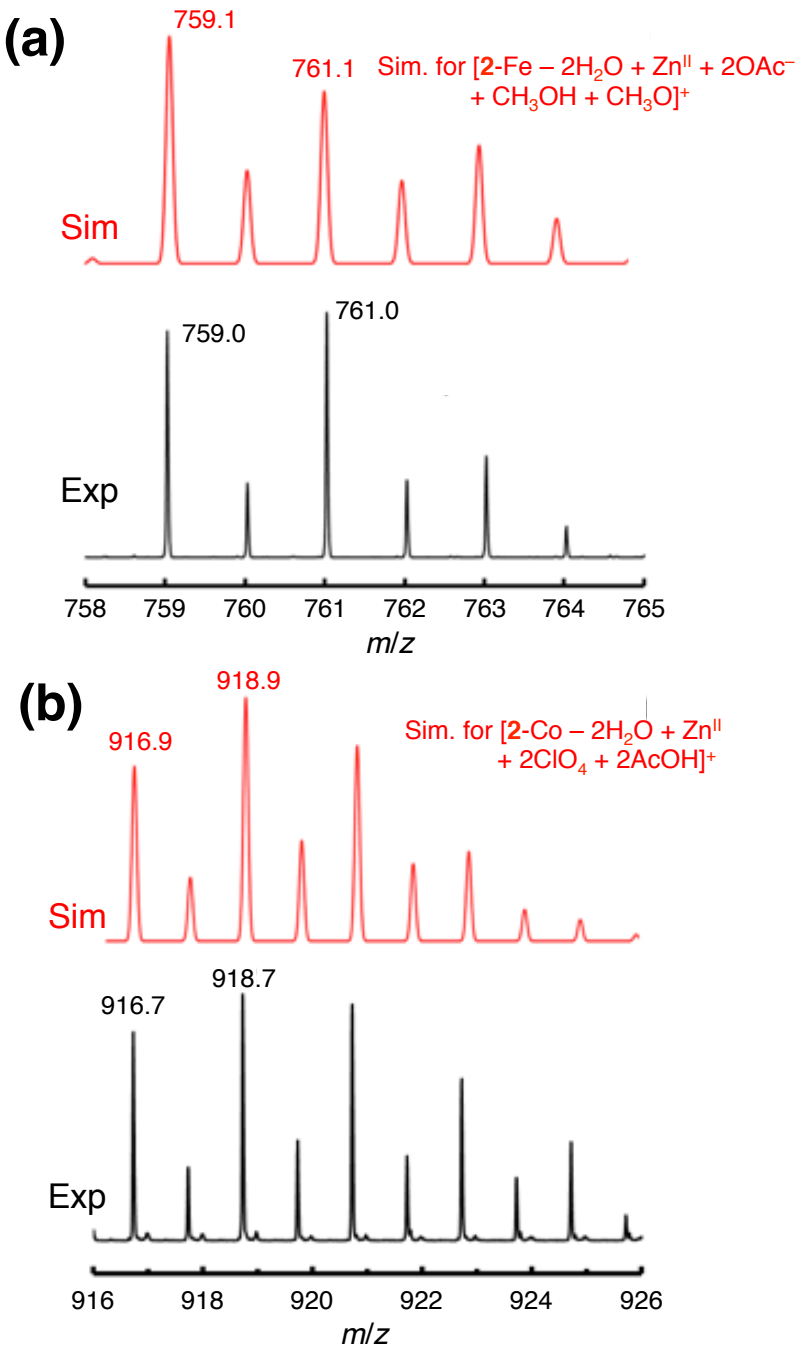

Fig. S8. (a) A peak cluster (black) assignable to Zn^{2+}-bound **2**-Fe (black) in the ESI-TO-MS spectrum of **2**-Fe in the presence of $Zn(OAc)_2$ (0.6 mM) in CH_3CN, and its simulation (red). (b) A peak cluster (black) assignable to Zn^{2+}-bound **2**-Co (black) in the ESI-TO-MS spectrum of **2**-Co in the presence of $Zn(OAc)_2$ (0.6 mM) in CH_3CN, and its simulation (red).

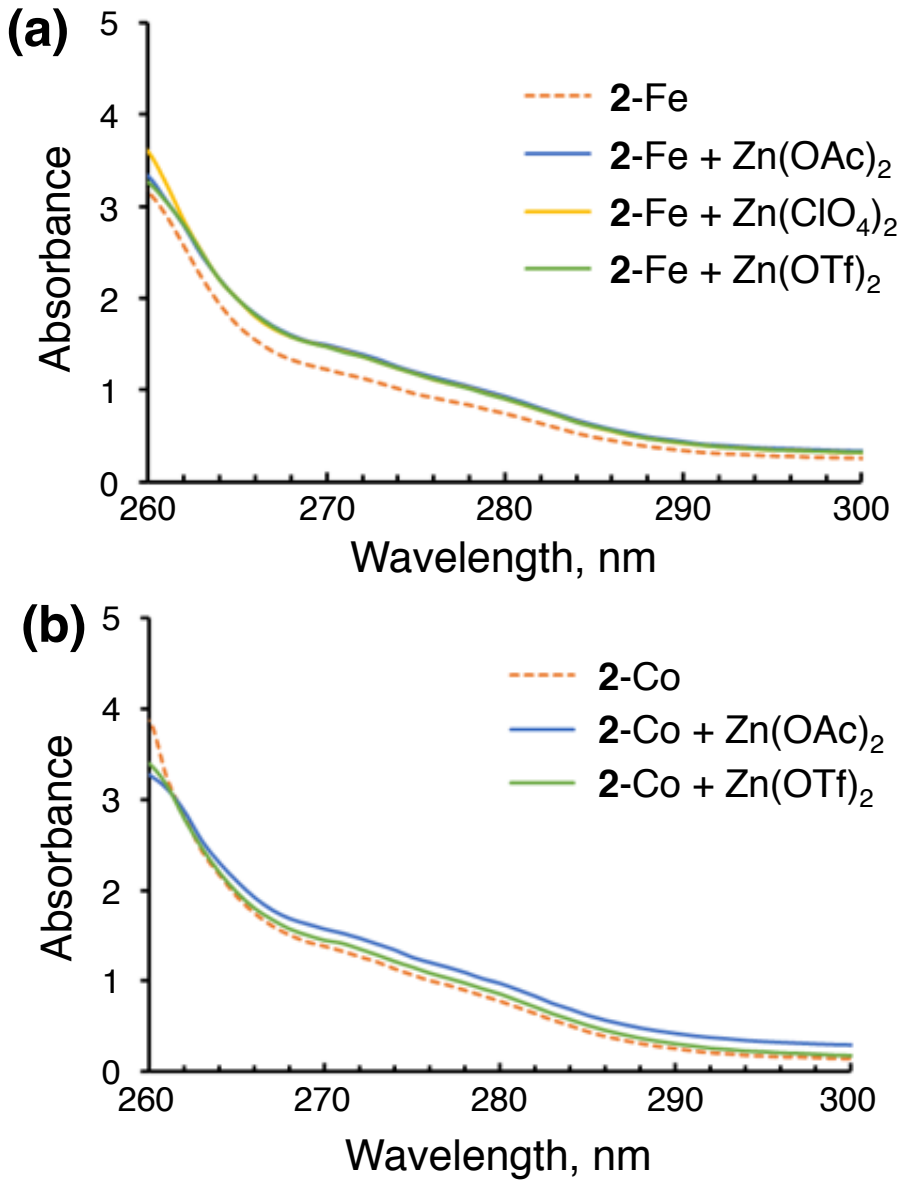

Fig. S9. (a) UV-vis spectral change of **2**-Fe (0.1 mM) in the absence (orange dotted line) and presence of various zinc salts (0.6 mM) as Lewis acid in a DMA/H_2O (9:1, v/v) mixed solution at room temperature. (b) UV-vis spectral change of **2**-Co (0.1 mM) in the absence (orange dotted line) and presence of various zinc salts (0.6 mM) as Lewis acid in a DMA/H_2O (9:1, v/v) mixed solution at room temperature.

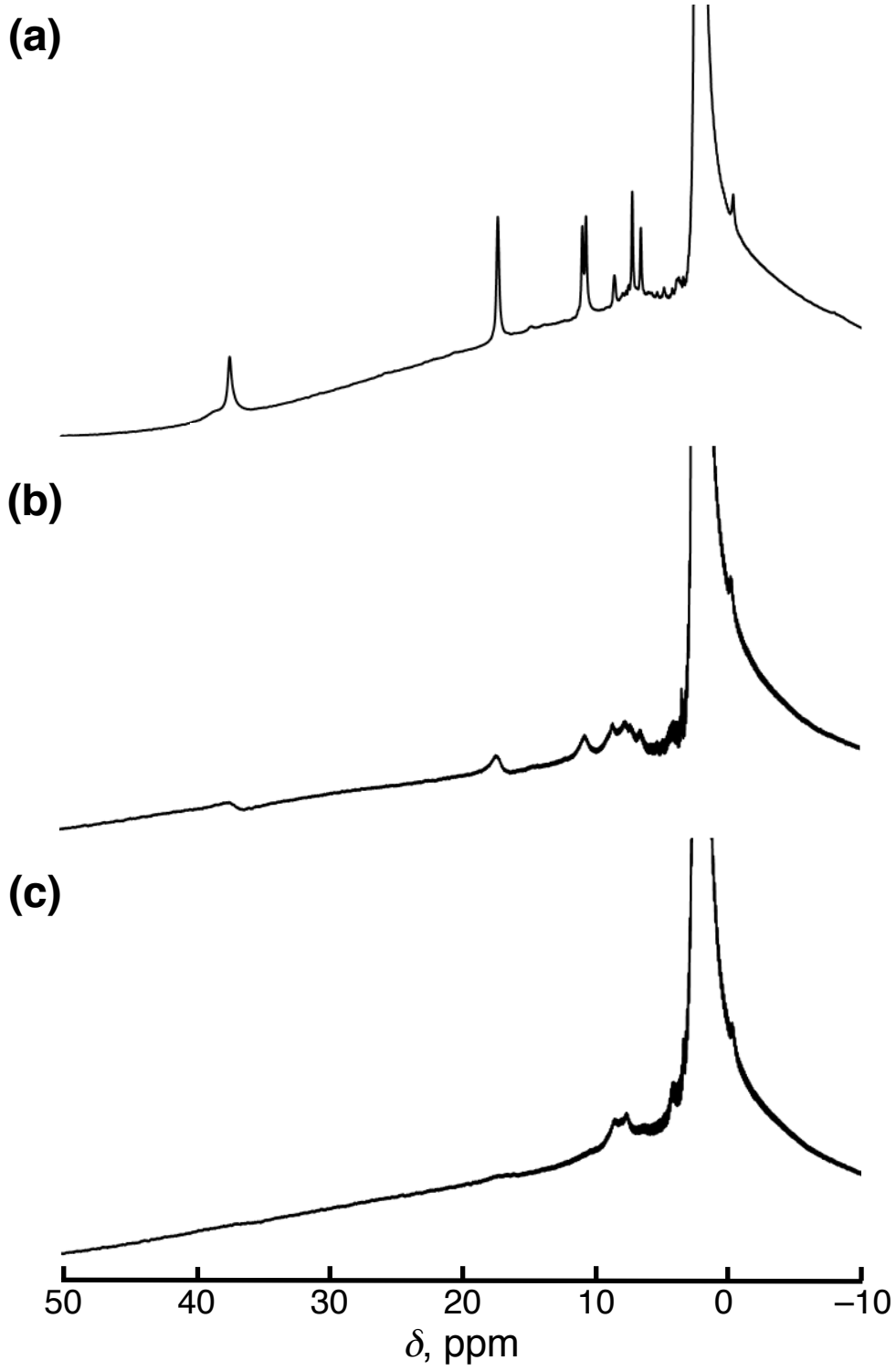

Fig. S10. ^{1}H NMR spectral change of [**2**-Co]$(ClO_4)_2$ (0.40 mM) at 300 K in CD_3CN by addition of $Zn(OAc)_2$: $[Zn(OAc)_2]$ = 0 (a), 0.40 (b), and 1.2 mM (c).

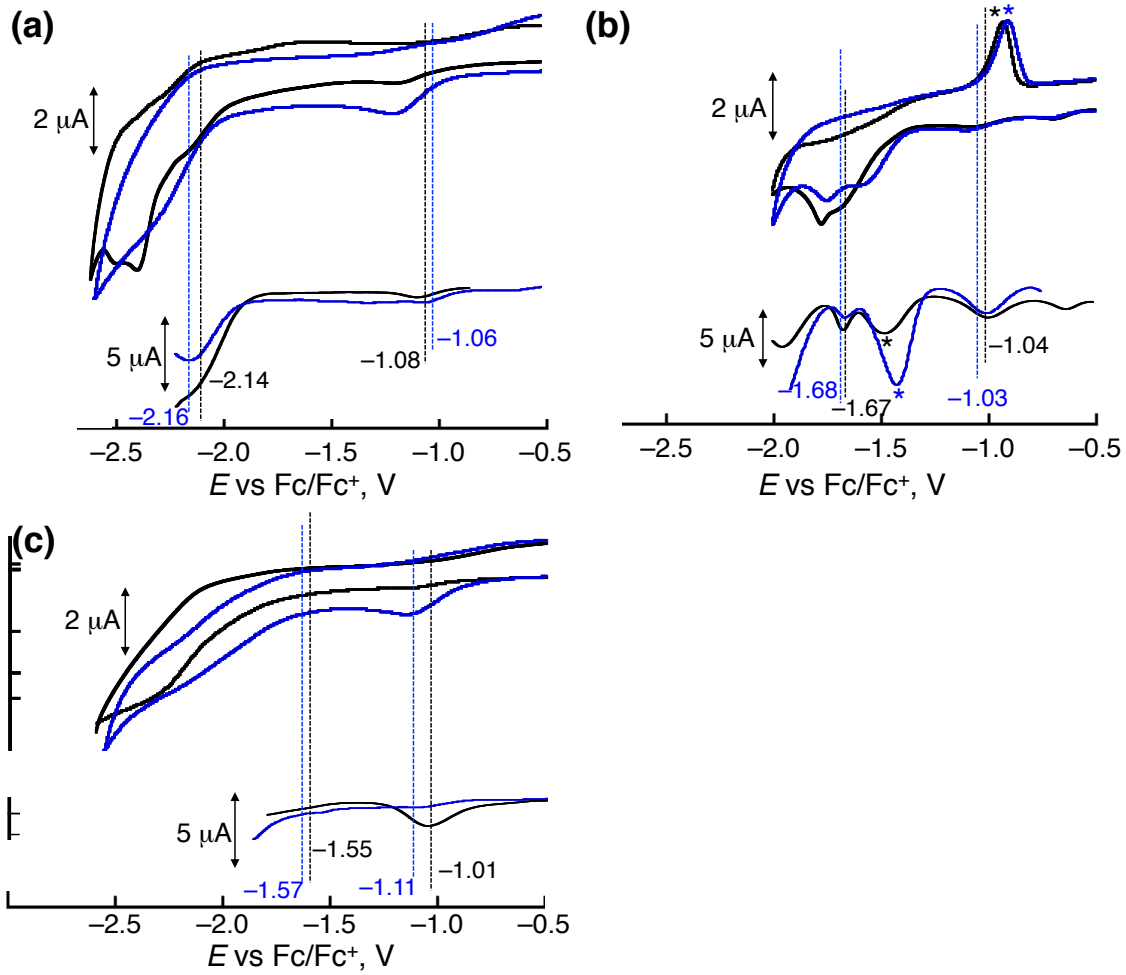

Fig. S11. CV and DPV traces of **2**-Mn (a), **2**-Fe (b) and **2**-Co (b) under Ar (black) and CO_2 atmosphere (blue) in a DMA/H_2O (9:1, v/v) solution containing 0.10 M $TBAPF_6$ as an electrolyte. [**2**-M] = 1.0 mM. * denotes an adsorption wave.

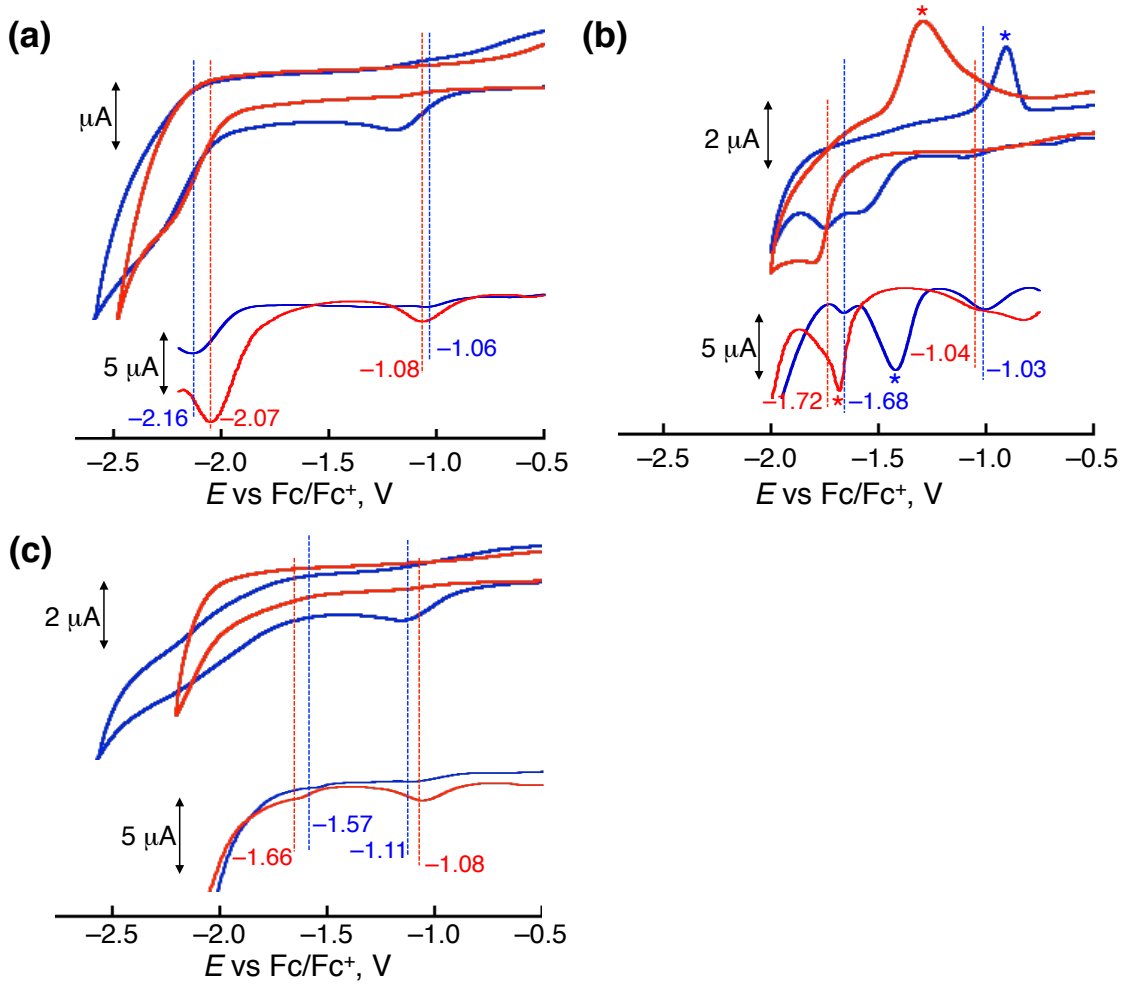

Fig. S12. CV and DPV traces of **2**-Mn (a), **2**-Fe (b) and **2**-Co (b) in the absence (blue) and presence (red) of $Zn(OAc)_2$ (0.6 mM) in a DMA/H_2O (9:1, v/v) solution containing 0.10 M $TBAPF_6$ as an electrolyte under CO_2 (red) atmosphere. [**2**-M] = 1.0 mM. * denotes an adsorption wave.

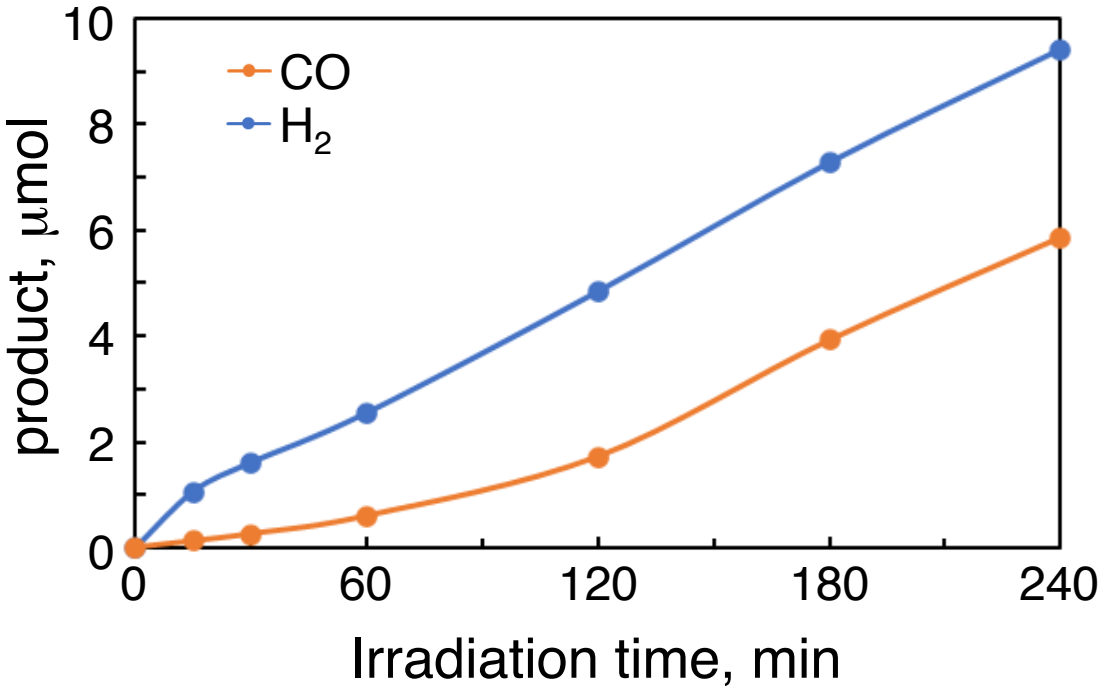

Fig. S13. Time courses of the CO (orange) and H_2 production (blue) in the photocatalytic reaction at room temperature under irradiation (λ_{centre} = 450 nm) and CO_2 atmosphere (1 atm) in a CH_3CN/H_2O (4.0 mL, 9:1 v/v) mixed solution, containing $[Ru(bpy)_3]^{2+}$ (0.10 mM), BIH (0.10 M) and **2**-Co (30 μM).

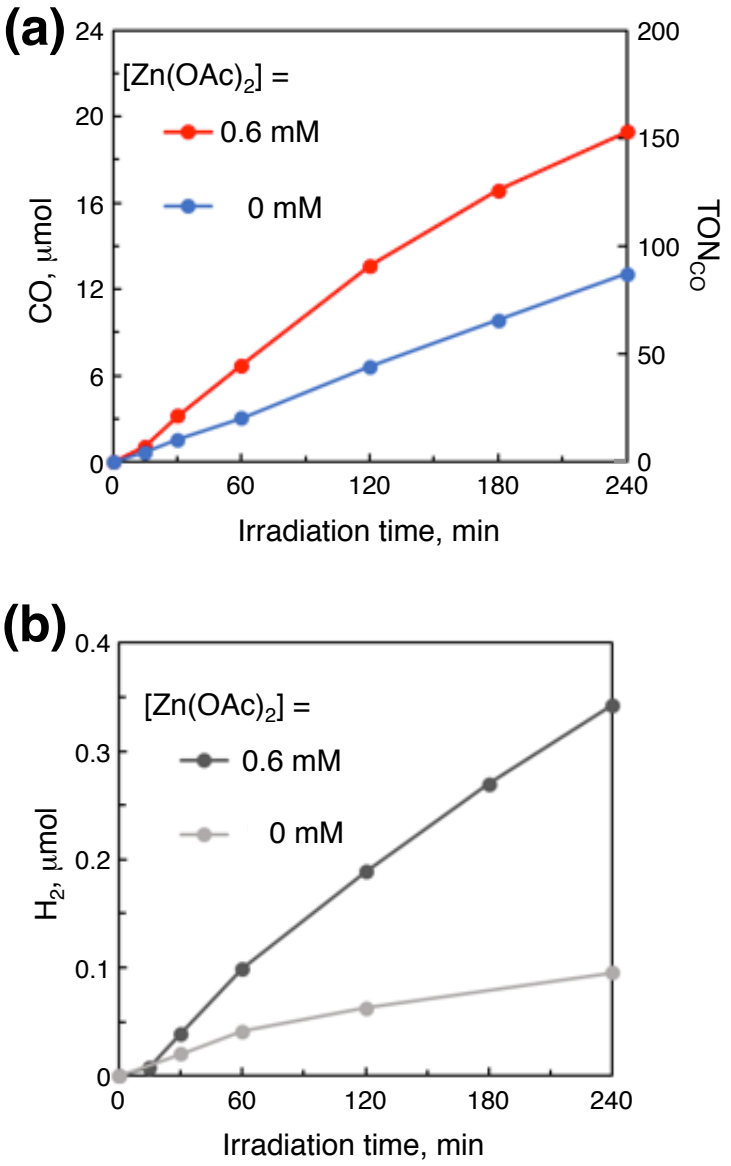

Fig. S14. Time courses of the CO (a) and H_2 production (b) in the photocatalytic reaction at room temperature under irradiation (λ_{centre} = 450 nm) and CO_2 atmosphere (1 atm) in a DMA/H_2O (4.0 mL, 9:1 v/v) mixed solution, containing $[Ru(bpy)_3]^{2+}$ (0.10 mM), BIH (0.10 M) and **2**-Mn (30 μM) in the absence (blue and grey circles) or presence (0.6 mM; red and black circles) of $Zn(OAc)_2$.

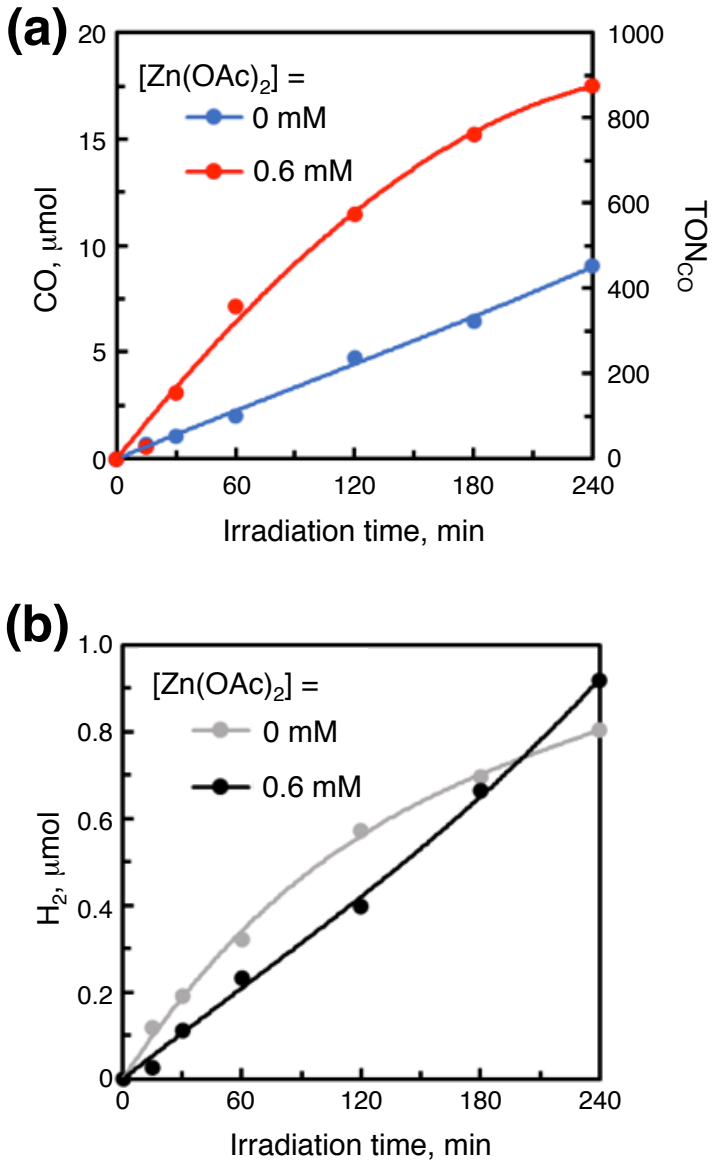

Fig. S15. Time courses of the CO (a) and H_2 production (b) in the photocatalytic reaction at room temperature under irradiation (λ_{centre} = 450 nm) and CO_2 atmosphere (1 atm) in a DMA/H_2O (4.0 mL, 9:1 v/v) mixed solution, containing $[Ru(bpy)_3]^{2+}$ (0.10 mM), BIH (0.10 M) and **2**-Mn (5 μM) in the absence (blue and grey circles) or presence (0.6 mM; red and black circles) of $Zn(OAc)_2$.

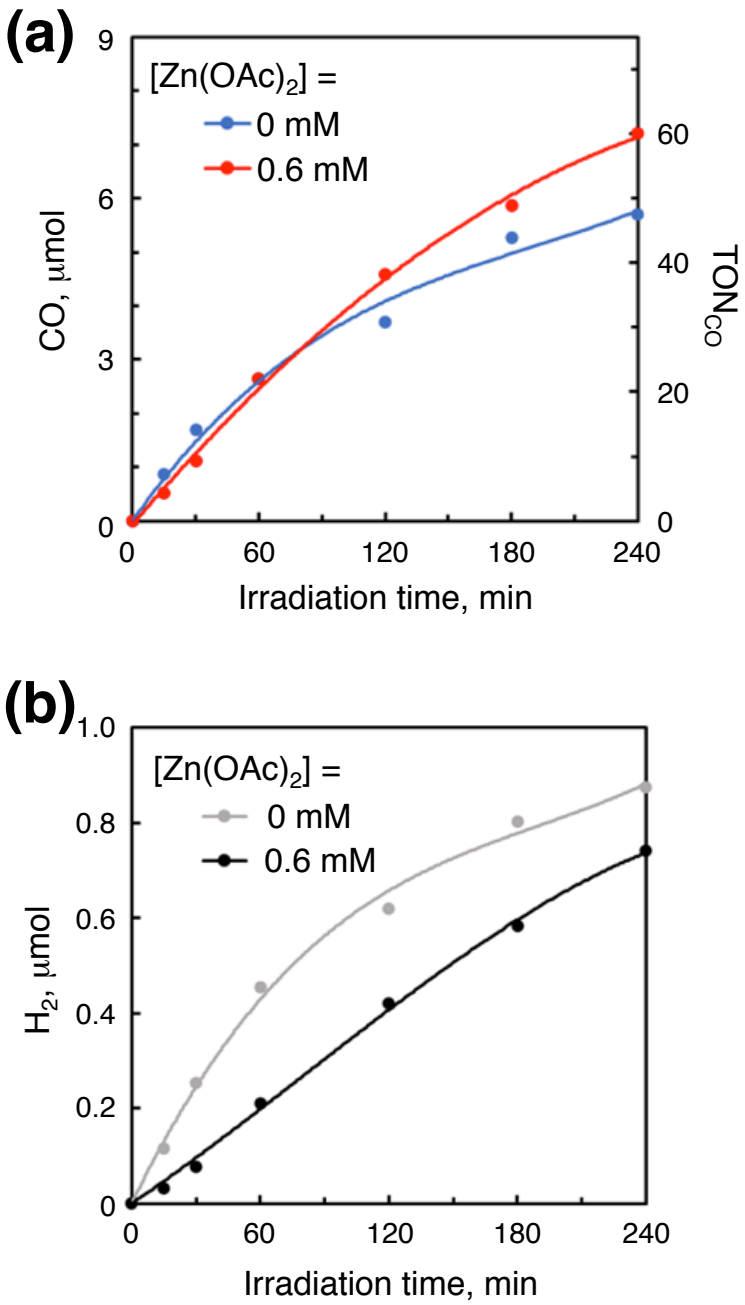

Fig. S16. Time courses of the CO (a) and H_2 production (b) in the photocatalytic reaction at room temperature under irradiation (λ_{centre} = 450 nm) and CO_2 atmosphere (1 atm) in a DMA/H_2O (4.0 mL, 9:1 v/v) mixed solution, containing $[Ru(bpy)_3]^{2+}$ (0.10 mM), BIH (0.10 M) and **1**-Mn (30 μM) in the absence (blue and grey circles) or presence (0.6 mM; red and black circles) of $Zn(OAc)_2$.

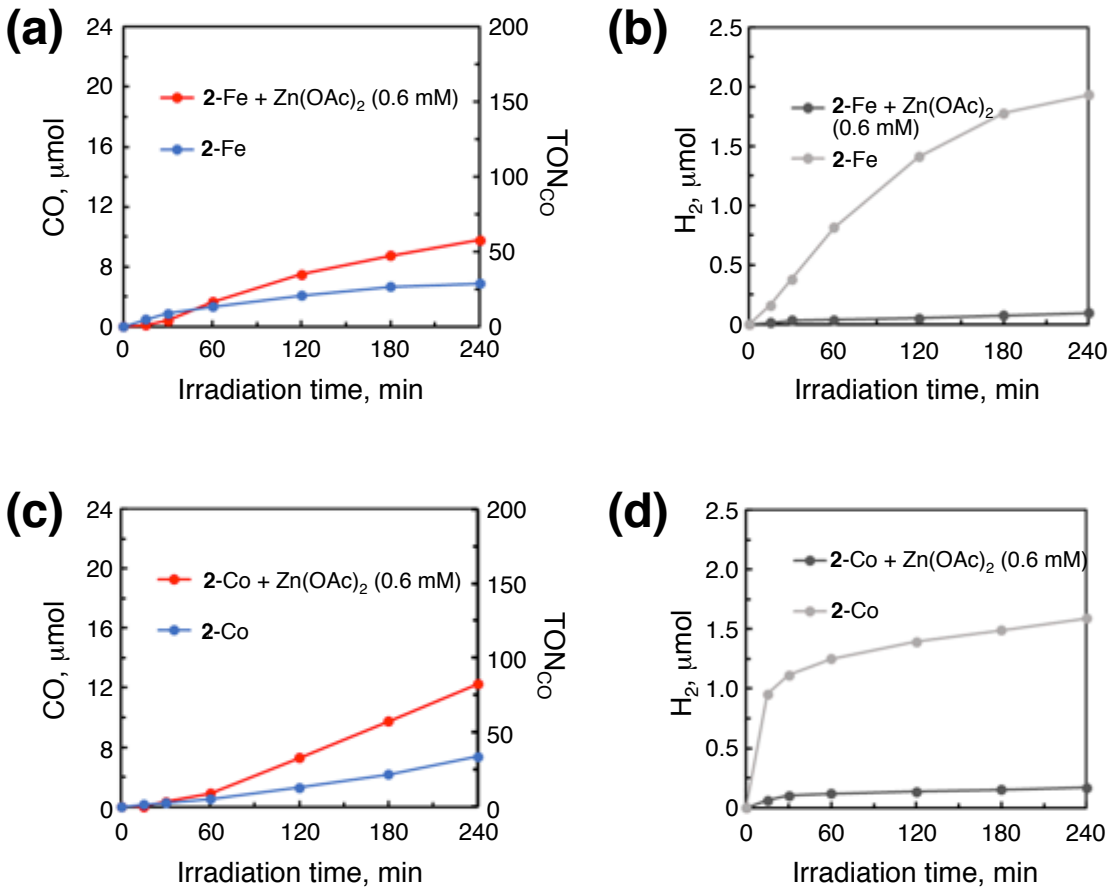

Fig. S17. Time courses of the CO (a and c) and H_2 production (b and d) in the photocatalytic reaction at room temperature under irradiation (λ_{centre} = 450 nm) and CO_2 atmosphere (1 atm) in a DMA/H_2O (4.0 mL, 9:1 v/v) mixed solution, containing $[Ru(bpy)_3]^{2+}$ (0.10 mM), BIH (0.10 M) and catalyst (30 μM) in the absence (blue and grey circles) or presence (0.6 mM; red and black circles) of $Zn(OAc)_2$. Catalyst: **2**-Fe (a and b), **2**-Co (c and d).

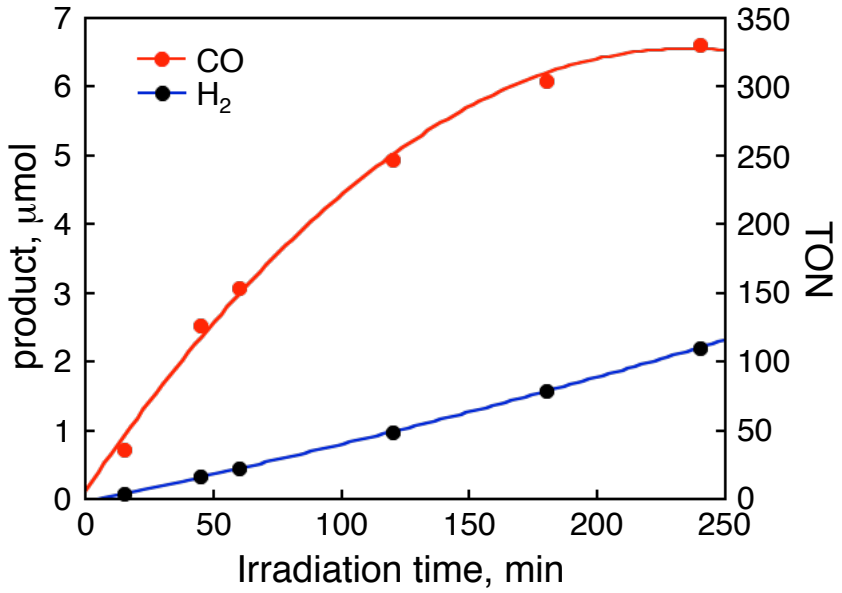

Fig. S18. Time courses of the CO (red) and H_2 production (black) in the photocatalytic reaction at room temperature under irradiation (λ_{centre} = 450 nm) and CO_2 atmosphere (1 atm) in a DMA/H_2O (4.0 mL, 9:1 v/v) mixed solution, containing $[Ru(bpy)_3]^{2+}$ (0.10 mM), BIH (0.10 M) and **2**-Fe (5 μM) in the presence (0.6 mM; red and black circles) of $Zn(OAc)_2$.

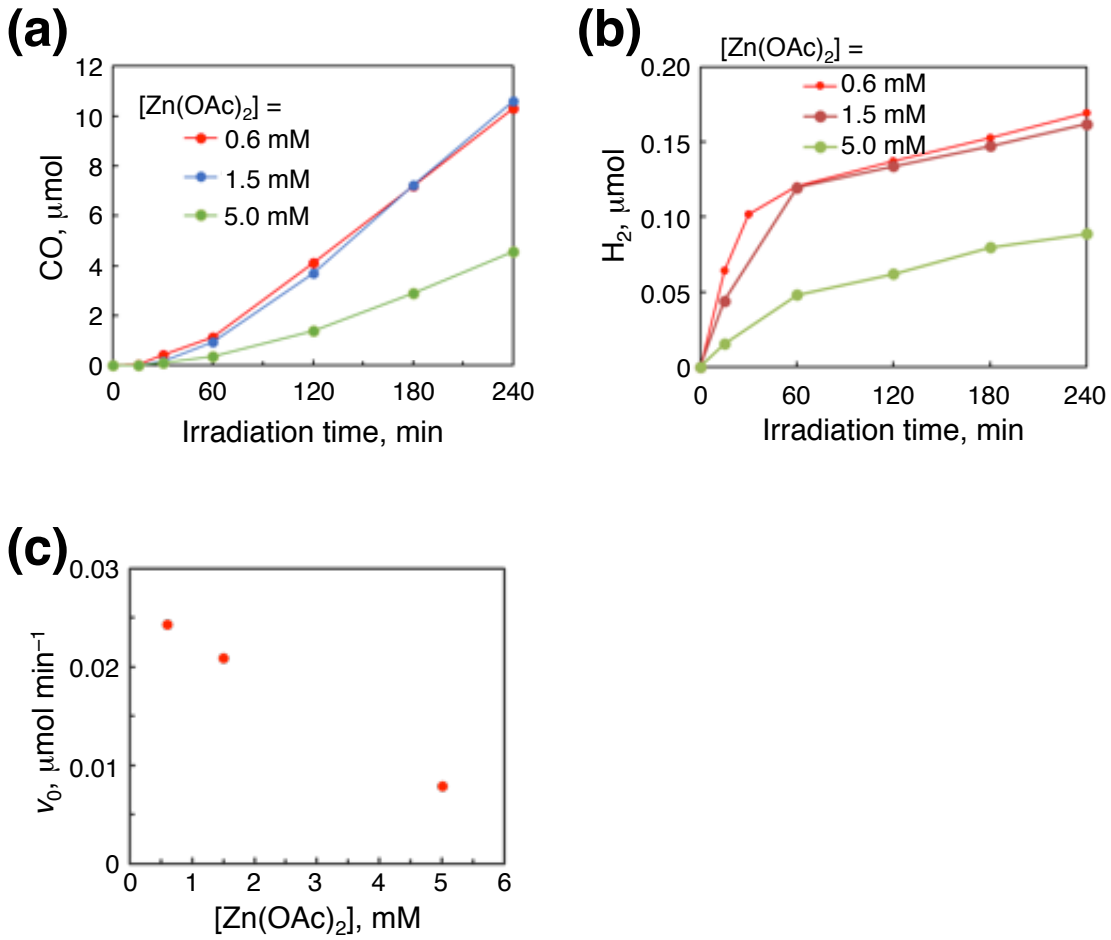

Fig. S19. Time sources of CO, (a) and H_2 evolution (b) in the photocatalytic CO_2 reduction under CO_2 atmosphere (1 atm) and irradiation (λ_{center} = 450 nm) to a DMA/H_2O (4.0 mL, 9:1 v/v) mixed solution containing **2**-Co (30 μM), $[Ru(bpy)_3]^{2+}$ (0.1 mM), BIH (0.1 M) and $Zn(OAc)_2$ (0.6–5.0 mM) at room temperature. (c) Dependence of the initial CO evolution rate, v_0, obtained from (a), on the concentration of $Zn(OAc)_2$.

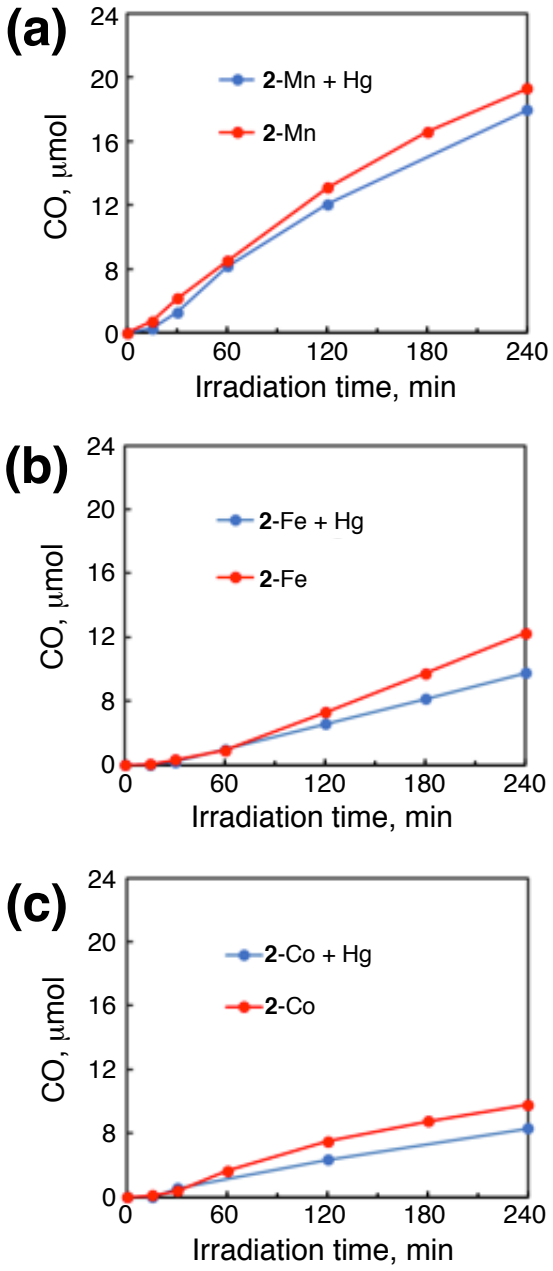

Fig. S20. Time courses of CO evolution in the photocatalytic reaction under CO_2 atmosphere (1 atm) and photoirradiation (λ_{center} = 450 nm) in a DMA/H_2O (9:1, v/v) mixed solution containing a catalyst (30 μM), **2**-Mn (a), **2**-Fe (b) and **2**-Co (c), $[Ru(bpy)_3]^{2+}$ (0.1 mM), BIH (0.1 M) and $Zn(OAc)_2$ (0.6 mM) in the absence (red circles) or presence (blue circles) of Hg drops at room temperature.

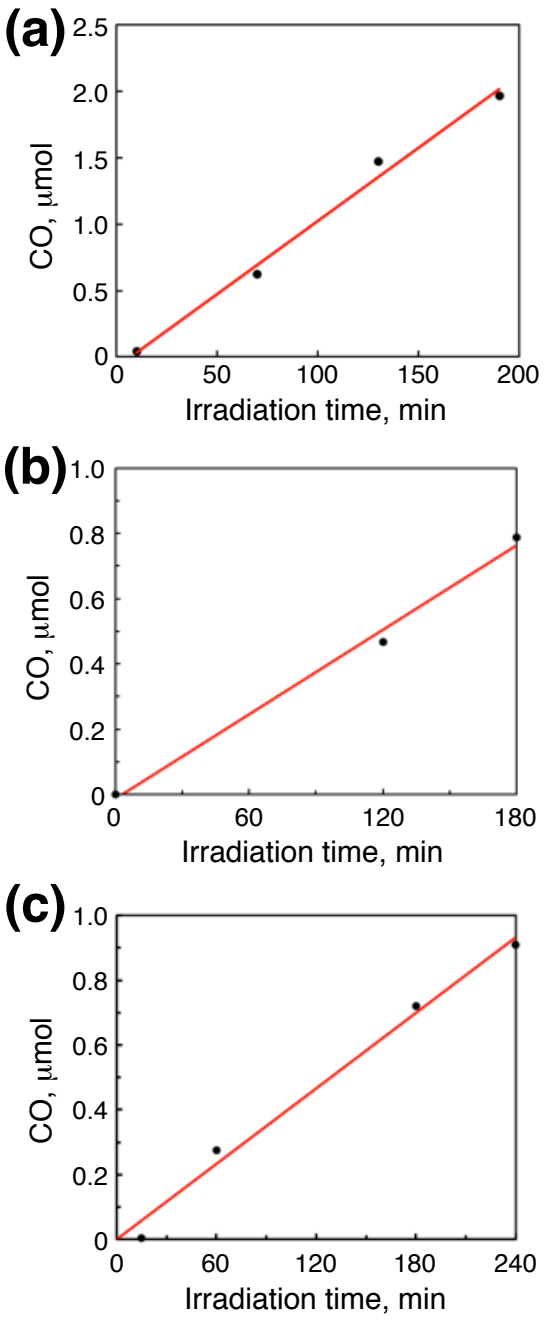

Fig. S21. Time course of CO evolution for the quantum yield determination by photoirradiation (λ_{center} = 450 nm) to a DMA/H_2O (9:1, v/v) mixed solution containing, a catalyst, $[Ru(bpy)_3]^{2+}$ (0.1 mM), BIH (0.1 M) and $Zn(OAc)_2$ (0.6 mM) under CO_2 atmosphere at room temperature. Catalyst: **2**-Mn (30 μM), (a), **2**-Fe (30 μM) (b), or **2**-Co (150 μM) (c).

Table S1. Selected bond distances and angles of **1**-Fe, **1**-Co (Solv = CH_3CN) and **1**-Mn

Compound	**1**-Fe[a]		**1**-Co (Solv = CH_3CN)	**1**-Mn
M–S1	2.243(1)	2.2337(9)	2.495(1)	2.623(3)
M–S2	2.232(1)	2.2488(9)	2.5003(9)	2.613(3)
M–N1	2.008(3)	2.011(2)	2.119(2)	2.238(6)
M–N2	2.009(2)	2.002(2)	2.124(2)	2.256(5)
M–X1 (Solv)	1.954(3) (X = N)	1.949(3) (X = N)	2.090(2) (X = N)	2.22(1) (X = O)
M–X2 (Solv)	1.944(3) (X = N)	1.948(3) (X = N)	2.115(3) (X = N)	2.121(7) (X = O)
∠N1-M-S1	84.79(9)	85.65(8)	80.79(6)	78.0(2)
∠S1-M-S2	90.61(4)	89.37(3)	86.64(3)	84.97(8)
∠S1-M-N2	85.40(7)	91.21(7)	93.98(7)	84.4(2)
∠S2-M-N2	90.88(8)	85.04(7)	80.76(7)	78.4(2)

[a] Two independent molecules of the cation moiety, $[Fe^{II}(bpet)(CH_3CN)_2]^{2+}$, are included in the asymmetric unit.

Table S2. Time course of the catalytic performance of **2**-Fe under its diluted conditions

Irradiation time, min	CO, μmol	H_2, μmol	Sel_{CO}, %
15	0.7283	0.0694	91.3
45	2.5265	0.3242	88.6
60	3.0799	0.4422	87.4
120	4.9412	0.9796	83.5
180	6.0966	1.5668	79.6
240	6.6174	2.2061	75.0

Conditions: $[Ru(bpy)_3]^{2+}$ (0.10 mM), [BIH] = 0.10 M, $[Zn(OAc)_2]$ = 0.60 mM, P_{CO2} = 1 atm, T = 298 K. Solvent: DMA/H_2O (9:1 v/v, 4.0 mL). Light source: LED centred at 450 nm. Catalyst = **2**-Fe (5 μM).

Table S3. Crystallographic Data of **1**-Fe, **1**-Co and **1**-Mn

	1-Fe	**1**-Co	**1**-Mn
		(Solv = CH_3CN)	
formula	$C_{18}H_{22}N_4S_2FeCl_2O_8$	$C_{18}H_{22}N_4S_2CoCl_2O_8$	$C_{14}H_{20}N_2S_2O_{10}MnCl_2$
formula wt	613.26	616.34	566.28
cryst syst	triclinic	monoclinic	triclinic
space group	$P\ \bar{1}$	$C2/c$	$P\ \bar{1}$
a, Å	12.063(2)	15.271(2)	10.581(7)
b, Å	12.378(2)	15.552(2)	11.018(7)
c, Å	16.823(3)	21.622(3)	11.389(13)
α, °	90.471(2)	90	109.060(9)
β, °	94.895(2)	105.223(2)	91.661(9)
γ, °	90.773(2)	90	118.443(6)
V, Å^3	2502.5(8)	4955.0(12)	1076.0(15)
Z	4	8	2
$R1(I > 2\sigma)$	0.0473	0.0430	0.1124
$wR2$(all)	0.1264	0.0962	0.2919
GOF	1.030	1.055	1.074